PHYSICAL REVIEW C **79**, 011301(R) (2009)

Spherical proton-neutron structure of isomeric states in ^{128}Cd

L. Cáceres,[1,2,*] M. Górska,[1] A. Jungclaus,[2,3] M. Pfützner,[4] H. Grawe,[1] F. Nowacki,[5] K. Sieja,[1] S. Pietri,[6,†] D. Rudolph,[7] Zs. Podolyák,[6] P. H. Regan,[6] E. Werner-Malento,[4,‡] P. Detistov,[8,§] S. Lalkovski,[8,9] V. Modamio,[2] J. Walker,[2] K. Andgren,[10] P. Bednarczyk,[1,11] J. Benlliure,[12] G. Benzoni,[13] A. M. Bruce,[9] E. Casarejos,[12] B. Cederwall,[10] F. C. L. Crespi,[13] P. Doornenbal,[1,14,‖] H. Geissel,[1] J. Gerl,[1] J. Gręboszz,[1,11] B. Hadinia,[10] M. Hellström,[7] R. Hoischen,[1,7] G. Ilie,[14,15] A. Khaplanov,[10] M. Kmiecik,[11] I. Kojouharov,[1] R. Kumar,[16] N. Kurz,[1] A. Maj,[11] S. Mandal,[17] F. Montes,[1,¶] G. Martínez-Pinedo,[1] S. Myalski,[11] W. Prokopowicz,[1] H. Schaffner,[1] G. S. Simpson,[18] S. J. Steer,[6] S. Tashenov,[1] O. Wieland,[13] and H. J. Wollersheim[1]

[1]*Gesellschaft für Schwerionenforschung (GSI), D-64291 Darmstadt, Germany*
[2]*Departamento de Física Teórica, Universidad Autónoma de Madrid, E-28049 Madrid, Spain*
[3]*Instituto de Estructura de la Materia, CSIC, Serrano 113 bis, E-28006 Madrid, Spain*
[4]*IEP, Warsaw University, PL-00681 Warsaw, Poland*
[5]*IReS, IN2P3-CNRS/University Louis Pasteur, F-67037, Strasbourg, France*
[6]*Department of Physics, University of Surrey, Guildford GU2 7XH, United Kingdom*
[7]*Department of Physics, Lund University, S-22100 Lund, Sweden*
[8]*Faculty of Physics, University of Sofia, BG-1164 Sofia, Bulgaria*
[9]*School of Engineering, University of Brighton, Brighton BN2 4GJ, United Kingdom*
[10]*KTH Stockholm, S-10691 Stockholm, Sweden*
[11]*The Henryk Niewodniczański Institute of Nuclear Physics, PAN, PL-31342 Kraków, Poland*
[12]*Universidade de Santiago de Compostela, E-15782 Santiago de Compostela, Spain*
[13]*INFN, Universitádegli Studi di Milano and INFN sezione di Milano, I-20133 Milano, Italy*
[14]*Institut für Kernphysik, Universität zu Köln, D-50937 Köln, Germany*
[15]*National Institute of Physics and Nuclear Engineering, Bucharest 76900, Romania*
[16]*Inter University Accelerator Centre, New Delhi, India*
[17]*University of Delhi, New Delhi, India*
[18]*LPSC, Université Joseph Fourier Grenoble 1, CNRS/IN2P3, Institut National Polytechnique de Grenoble, F-38026 Grenoble Cedex, France*

(Received 24 September 2008; published 7 January 2009)

The γ-ray decay of isomeric states in the even-even nucleus ^{128}Cd has been observed. The nucleus of interest was produced both by the fragmentation of ^{136}Xe and the fission of ^{238}U primary beams. The level scheme was unambiguously constructed based on $\gamma\gamma$ coincidence relations in conjunction with detailed lifetime analysis employed for the first time on this nucleus. Large-scale shell-model calculations, without consideration of excitations across the $N = 82$ shell closure, were performed and provide a consistent description of the experimental level scheme. The structure of the isomeric states and their decays exhibit coexistence of proton, neutron, and strongly mixed configurations due to $\pi\nu$ interaction in overlapping orbitals for both proton and neutron holes.

DOI: 10.1103/PhysRevC.79.011301 PACS number(s): 21.60.Cs, 23.20.Lv, 23.35.+g, 27.60.+j

The development of the first generation radioactive beam facilities over the last decade has allowed access to experimentally very exotic nuclei with extreme proton-to-neutron ratios. Neutron-rich nuclei close to the doubly magic nucleus $^{132}_{50}$Sn$_{50}$ are relevant both for nuclear structure studies and for their implication for r-process nucleosynthesis. Hartree-Fock-Bogoliubov (HFB) calculations with the Skyrme force predict a reduction of the size of the $N = 82$ neutron shell gap when approaching $Z = 40$ [1]. This effect has been attributed to a reduction of the spin-orbit coupling strength caused by the strong interaction between bound orbitals and low-j continuum states. This is due to a large diffuseness of the outer neutron distribution and its influence on the central potential in exotic nuclei with large neutron excess. Dillmann *et al.* [2] pointed out that the experimental Q_β value of ^{130}Cd, only two proton-holes below ^{132}Sn, was better reproduced by those mass models that included "shell quenching" at $N = 82$ [3,4]. Moreover, the flattening of the Cd yrast 2^+ systematics from ^{126}Cd to ^{128}Cd, two-proton holes and four- and two-neutron holes with respect to ^{132}Sn, respectively, and the indication of a low lying 2^+ state in ^{130}Cd [5] have been interpreted as indirect evidence of the reduction of the $N = 82$ neutron shell gap

*L.Caceres@gsi.de
†Present address: Gesellschaft für Schwerionenforschung (GSI), D-64291 Darmstadt, Germany.
‡Present address: IF PAN, Warsaw, Poland.
§Present address: Universidad de Salamanca, E-37008 Salamanca, Spain.
‖Present address: RIKEN, Japan.
¶Present address: University of Michigan, MSU, USA.

already at $Z = 48$. In the same work it has been suggested that some collectivity persists in those very neutron-rich Cd nuclei approaching the neutron shell closure. The recently reported isomeric γ decay in ^{130}Cd [6] that unambiguously established the 2^+ excitation energy at 1325 keV concluded that there is no evidence for shell quenching at that atomic number. This conclusion is confirmed in a forthcoming publication where the measurement of a core excited isomeric state in ^{131}In [7] is reported. However, the low value of the 2^+ excitation energy in ^{128}Cd is still an open question. Beyond-mean-field calculations [8] attribute the anomalous behavior of the $E(2^+)$ in the Cd chain to the presence of quadrupole collectivity close to the $N = 82$ shell gap as suggested in Refs. [5,9,10]. To shed light on the structural aspects of the nucleus discussed above, a study of high-spin isomers and their decay has been performed. Recently, based on a similar experimental approach, however without any time correlations, a level scheme for the near-yrast states of ^{128}Cd has been proposed [11].

Because high-spin isomeric states in the ^{132}Sn region can be populated in fragmentation and/or fission reactions, the ^{128}Cd nuclei in this experiment were produced both in fragmentation of a ^{136}Xe primary beam at 750 MeV/u and average intensity $\sim 7.4 \times 10^8$ ions/s and in fission of a ^{238}U primary beam at 650 MeV/u and average intensity $\sim 2.7 \times 10^8$ ions/s delivered by the SIS accelerator complex of GSI Darmstadt, Germany. The Xe and U primary beams impinged on ^{9}Be targets of 4 g/cm^2 and 1 g/cm^2 thickness, respectively. The reaction products were separated by means of the $B\rho$-ΔE-$B\rho$ method in the FRagment Separator (FRS) at GSI [12] operated in achromatic mode. The identification was performed on an event-by-event basis by measuring the time of flight between two scintillator detectors placed in the intermediate and the final focal planes of the FRS, the energy loss in two ionization chambers, and the magnetic rigidity of the ions. Figure 1 shows an example identification plot for the nuclei produced in the fragmentation reaction with the FRS set to optimize the transmission of ^{130}Cd ions. In total 3.29×10^5 ^{128}Cd nuclei were identified. The ions were slowed down in an Al degrader and stopped in a plastic stopper positioned at the final focal plane of the FRS. The isomeric states populated

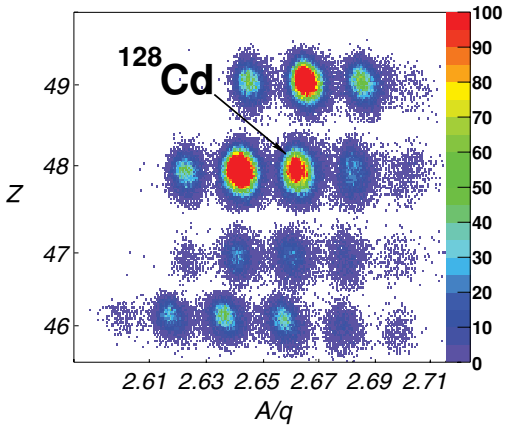

FIG. 1. (Color online) Particle identification plot of the ion production of 25% of the data from the fragmentation of a ^{136}Xe beam.

in these reactions with a half-life long enough to survive the flight through the FRS (≈300 ns) come to rest in the stopper and can be identified by their characteristic γ-ray emissions. The RISING Ge array placed in close geometry around the stopper was used to measure the γ radiation from the isomeric decays. The array consists of 15 Ge cluster detectors [13] from the former EUROBALL [14] spectrometer. By requiring a coincidence between the identified ion and the detected γ radiation over a range from 0 to 23 μs after implantation, the detected γ rays can be unambiguously assigned to the isomeric decay of one particular isotope. The time was measured in two independent electronic circuits: An analog branch with a time increment/scale of 0.7 ns/ch and a digital branch with 25 ns/ch. The γ-ray energy measurement ranged from 30 keV to 6 MeV. The high efficiency [15] and granularity of this Ge array in combination with the particle identification of the FRS makes this setup a unique tool for γ-ray spectroscopy studies. The delayed γ-ray singles spectrum measured following the implantation of ^{128}Cd is shown in Fig. 2(a). All previously reported transitions [5,11] are visible and in addition two strong lines at 69 and 1224 keV are observed for the first time. The level scheme proposed in Ref. [11] will not be considered further in view of the analysis presented in this work which includes $\gamma\gamma$ coincidences (Fig. 2) and half-life analysis (Figs. 3 and 4). Based on these results the inferred level scheme shown in Fig. 5 is discussed. The γ-ray energies, their relative intensities normalized to the most intense 646 keV transition, and the half-lives of the isomeric states observed in ^{128}Cd in this experiment are summarized in Table I.

In the $\gamma\gamma$ coincidence analysis with an open time condition ($\Delta t = 23.254$ μs) it was found that all strong γ rays seen in Fig. 2(a) belong to the main cascade with the exception of the 1224 keV transition, which is not observed in coincidence with the 440 and 785 keV lines. The coincidence spectrum gated on the latter is shown in Fig. 2(b). The 785 and 646 keV transitions were assigned from β-decay studies in Ref. [5] to form the $4^+ \rightarrow 2^+ \rightarrow 0^+$ cascade. The ordering of these two transitions is now unambiguously confirmed by the new $\gamma\gamma$ coincidence information. The 440 keV line was placed feeding the 4^+ state and decaying from the 1871 keV level. Furthermore, a $\gamma\gamma$ matrix was constructed requiring the time difference between the two coincident γ rays to be less than 125 ns. The spectrum obtained from this matrix by gating on the 238 keV transition shows a strong reduction in the intensity of the 646, 785, 440, and 1224 keV γ rays when compared to the 538 keV γ peak as visible in Fig 2(c). Corresponding coincidence relations were found by gating on the 538 and 69 keV peaks, with respect to the 238 keV intensity, and the other lines. This observation indicates the existence of at least two isomeric states with different lifetimes in ^{128}Cd. The time distributions of the γ rays below the 1871 keV level show indeed two decay components while the 69, 238, and 538 keV transitions decaying from the state at 2714 keV show only a single exponential decay, resulting in an isomeric half-life of 3.56(6) μs for this state (Fig. 3). The half-life of the state at 1871 keV was extracted from the γ versus relative γ-ray time difference matrix between the 238 keV transition and the γ lines below that state. Under this condition, the time distributions of the 648, 785, 1220, and 440 keV γ rays show

TABLE I. Experimental results and deduced spin and parity assignments for the excited states in ^{128}Cd. The γ intensities are normalized to the 646 keV transition.

E_i (keV)	$T_{1/2}$ (μs)	$I_i^\pi \rightarrow I_f^\pi$	E_γ (keV)	I_γ (%)	$\alpha_{\rm exp}$
646		$2^+ \rightarrow 0^+$	645.8(2)	100(5)	
1430		$4^+ \rightarrow 2^+$	784.6(1)	90(5)	
1871	0.270(7)	$(5^-) \rightarrow (4^+)$	440.0(3)	84(4)	
		$(5^-) \rightarrow (2^+)$	1224.0(6)	11(1)	
2108	0.012(2)[a]	$(7^-) \rightarrow (5^-)$	237.9(5)	39(2)	
2195		$(6^+) \rightarrow (4^+)$	765.0(3)	1.2(2)	
2646		$(8^+) \rightarrow (7^-)$	537.6(2)	47(3)	
		$(8^+) \rightarrow (6^+)$	450.4(3)	1.8(3)	
2714	3.56(6)	$(10^+) \rightarrow (8^+)$	68.7(1)	5.2(5)	6.38(86)[b]

[a]Extracted from the energy versus relative time matrix gated on the 538 keV transition.
[b]Extracted from the $\gamma\gamma$ matrix gating on the 238 keV transition.

a single exponential decay yielding a half-life of 270(7) ns for the isomeric state. This type of analysis also allowed us to determine the ordering of the 538 and 238 keV transitions. The time distribution of the 238 keV line with respect to the 538 keV transition exhibits a Gaussian shape with an exponential tail. The centroid shift method [16] and the least squares fit of the exponential component result in a half-life of 12(2) ns for the level at 2108 keV as shown in Fig. 4.

In addition to the strong γ rays mentioned above, two more weak transitions at 450 and 765 keV [Fig. 2(d)] are observed in coincidence with the 646 and 785 keV lines and are not present in the 538 keV γ-ray gate. The 450 keV transition was placed as preceding the one with 765 keV based on the weak coincidence relations of the 450 keV γ peak with the 238 and 440 keV transitions. These two γ rays are not in coincidence with the 765 keV transition. The 450 and 765 keV transitions form a parallel branch with an intermediate level at 2195 keV feeding the 4^+ state at 1430 keV. Their time distributions corroborate a one component fit to the decay of the 2714 keV level. The sum energy of the 538, 238, and 440 keV transitions is equal to that of 450 and 765 keV lines forming a state at 2646 keV.

The spin and parity assignment to the excited states is based on the electromagnetic transitions probabilities, relative intensity balance, and inferred conversion coefficients. The isomeric state at 1871 keV decays mainly by a 440 keV $E1\,\gamma$ ray to the 4^+ level with $B(E1;(5^-) \rightarrow 4^+) = 9.74(61) \times 10^{-9}$ W.u. and a parallel branch to the 2^+ by the

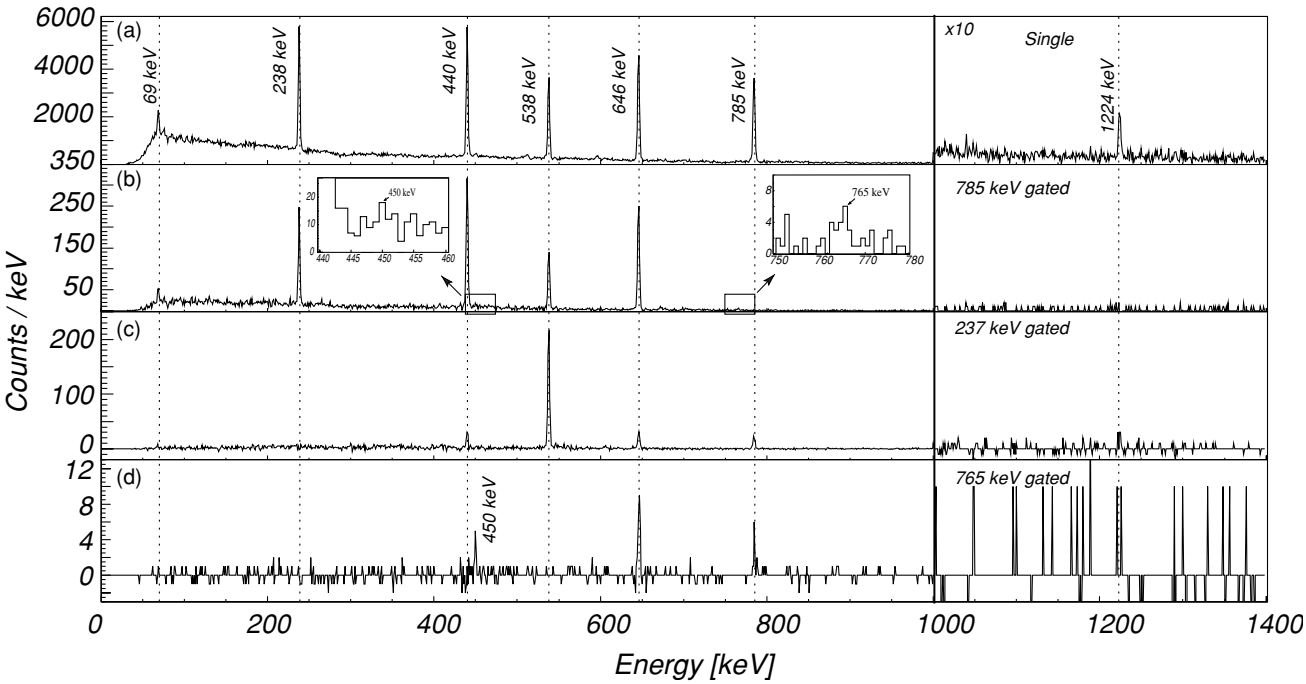

FIG. 2. (a) Singles γ-ray spectrum in coincidence with implanted ^{128}Cd ions. (b) Spectrum from the $\gamma\gamma$ matrix gated by the 785 keV transition with an open time condition applied ($\Delta t = 23.25$ μs). (c, d) Spectra obtained from the $\gamma\gamma$ matrix gated by the 238 and 765 keV transitions with the condition that the time difference between coincident γ rays is less than 125 ns, respectively.

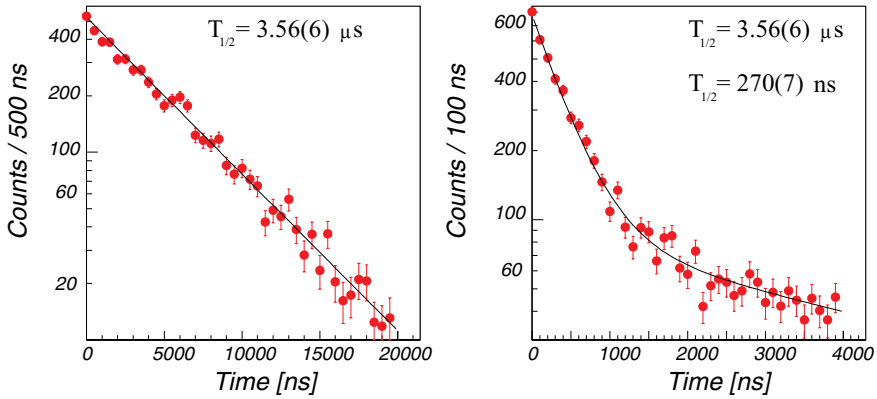

FIG. 3. (Color online) Time distribution relative to the ion implantation of the 238 keV (left) and 646 keV (right) γ transitions.

1224 keV $E3\,\gamma$ line with $B(E3;(5^-)\rightarrow 2^+) = 0.125(13)$ W.u. This $E3$ strength is comparable to the value $B(E3;7^-\rightarrow 4^+) = 0.133$ W.u. in ^{128}Sn [17] four-neutron holes in the doubly magic ^{132}Sn. An $E4$ character for the 1224 keV transition would not account for the experimental half-life; therefore, $I^\pi = (5^-)$ is assigned to the 1871 keV level. The multipolarity assignments for the 238, 450, 538, and 765 keV transitions are based on the following arguments. The 2108 keV isomeric state decays by the 238 keV transition with $B(E2;(7^-)\rightarrow(5^-)) = 1.5(3)$ W.u. strength, a value comparable with the $E2$ strength of a corresponding transition in the isotone ^{130}Sn [18]. The 2646 keV level decays by the emission of a 538 keV γ ray to the 2108 keV level and via a weak 450 keV transition to the 2195 keV state. The $B(E1;8^+\rightarrow 7^-) > 3.5\times 10^{-6}$ W.u. strength in ^{130}Sn [18] would correspond to a half-life of $<$0.5 ns for the 2646 keV state that cannot be excluded from our data. Within the experimental sensitivity the 538 keV transition is emitted promptly after the 69 keV γ ray. Because the spin difference between the 1430 and 2646 keV levels is $4\hbar$, both the 450 and 765 keV γ rays must be $E2$ transitions. The assignment of a higher multipolarity to any of those transitions would lead to a half-life longer than 50 μs for the 2195 or 2646 keV states. The latter is therefore assigned to $I^\pi = (8^+)$. The exchange of the spin and parity for the 2108 and 2195 keV levels would be at variance with the nonobservation of a 325 keV transition feeding the 1871 keV state. Therefore $I^\pi = (7^-)$ is assigned to the 2108 keV level and $I^\pi = (6^+)$ to the excited state at 2195 keV. The isomeric state at 2714 keV excitation energy was attributed spin and parity (10^+). It decays by a 69 keV $E2$ transition of 0.39(1) W.u. strength to the 2646 keV level. The experimental conversion coefficient for this γ ray was extracted by intensity balance arguments to be 6.38(86) in agreement with the theoretical value of $\alpha_{\rm tot}(E2) = 5.9$, thus corroborating this assignment.

The experimental data were compared to the results of large-scale shell-model (LSSM) calculations performed in a model space based on a ^{78}Ni core, comprising the proton $\pi(p_{3/2}, p_{1/2}, f_{5/2}, g_{9/2})$ and neutron $\nu(g_{7/2}, s_{1/2}, d_{5/2}, d_{3/2}, h_{11/2})$ orbitals. The effective interaction was derived from the CD-Bonn nucleon-nucleon potential [19] using G-matrix theory and adapted to the model space using many-body perturbation techniques [20]. Monopole corrections were applied to reproduce correctly the excitation energies of the neutron-rich nuclei below ^{132}Sn [21]. In particular, the evolution of the $1/2^-$ and $9/2^+$ proton doublet along the

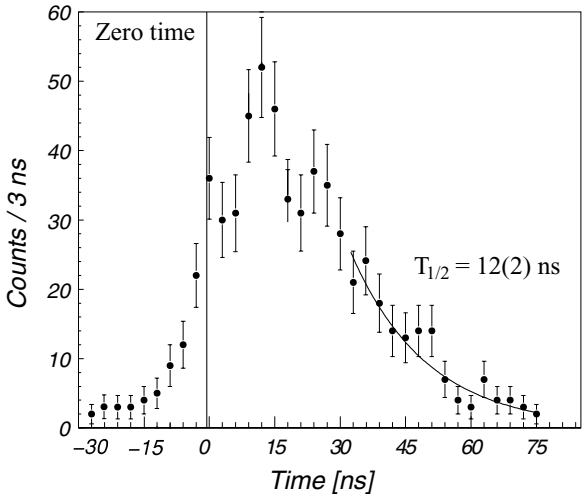

FIG. 4. Time distribution of the 238 keV line with respect to the 538 keV transition. The curve represents the result of the single exponential fit.

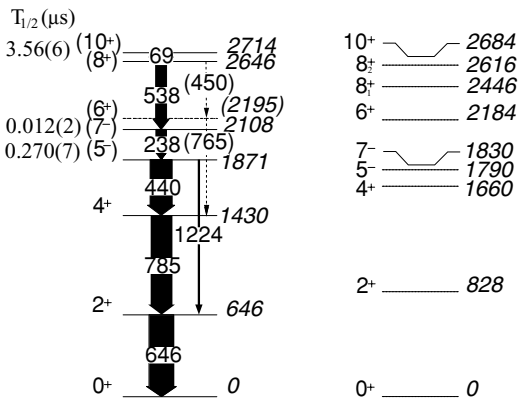

FIG. 5. Comparison of the deduced experimental level scheme for the isomeric deexcitation of ^{128}Cd (left) with shell model calculations (right).

indium chain and the neutron level schemes along the tin chain were reproduced. Because the adjustment of the monopole component of the interaction is part of a general shell model interaction study of the ^{78}Ni to ^{132}Sn model space [22], no further modifications specific for ^{128}Cd were applied. The calculations were performed with the codes ANTOINE and NATHAN [23]. Electromagnetic transition rates were calculated with a standard common polarization charge of 0.5 e for both protons and neutrons.

In Fig. 5 the experimental level scheme is compared to the LSSM calculations. The overall agreement between theory and experiment is satisfying in view of the fact that the spectrum is *a priori* rather complex with the coexistence of proton and neutron states. In particular, the high lying 8_2^+ and 10^+ states have predominant $h_{11/2}^{-2}$ neutron character (cf. ^{130}Sn) and are correctly located with respect to the $0^+ - 8_1^+ g_{9/2}^{-2}$ and $4^-, 5^-, g_{9/2}^{-1} p_{1/2}^{-1}$ proton multiplets (cf. ^{130}Cd). The shift in the excitation energies of the 2^+ and 4^+ states reveals the ground-state sensitivity to the mixing between the $\pi g_{9/2}$ and $\pi p_{1/2}$ proton configuration. An additional binding energy added to the $p_{1/2}$ single particle orbital would reduce the mixing and bring the results in agreement for the 2^+ and 4^+ states, however, at the cost of spoiling the location of the 5^- level. The latter with a predominant $\pi g_{9/2}^{-1} p_{1/2}^{-1}$ proton configuration (70%) is well reproduced in the calculation, whereas a slight discrepancy concerns the 7^- level dominated by the $(d_{3/2})^{-1}(h_{11/2})^{-1}$ neutron configuration that can be possibly traced back to the $\pi g_{9/2} \nu d_{3/2}$ monopole. The 6^+ has a mixed configuration proton-neutron wave function, which explains why it is populated from the neutron 8_2^+ and lies well below the proton 8_1^+ state, which is not seen in experiment (see below). Excellent agreement is, however, found for the energy of the isomeric 10^+ state. It appears to be formed mainly (86%) by the two maximum aligned neutron holes in the $h_{11/2}$ orbital and decays by an $E2$ transition to the 8_2^+ state dominated as well by the two-neutron hole configuration. The calculated 8_1^+ state at energy of 2446 keV is found to have a pronounced (64%) proton component that explains why it is not populated in the isomeric decay of the neutron 10^+. The $E2$ theoretical transition rates of $B(E2; 10^+ \rightarrow 8_2^+) = 0.59$ W.u. and $B(E2; 7^- \rightarrow 5^-) = 0.83$ W.u. agree well with the experimental values 0.39(1) W.u. and 1.5(3) W.u., respectively. The $B(E2; 10^+ \rightarrow 8_1^+) = 0.15$ W.u., though smaller by a factor of four compared to the transition to the 8_2^+, matches nonobservation only if the two 8^+ states are experimentally close in energy.

Summarizing, three isomeric states have been identified with the RISING Ge array in combination with the event-by-event particle identification by the FRS. The $\gamma\gamma$ coincidence and lifetime analysis allowed the construction of the level scheme populated following decays from isomeric states in ^{128}Cd. The experimental data indicate that the isomeric decay pattern is selective to the structure of the populated states and their leading π or ν configuration. This conclusion is further supported by comparison to LSSM calculations that yield an overall good agreement and additionally strengthen the spin and parity assignments. The deviations in level energies between experiment and shell model at intermediate spins reveal the need for a further adjustment of the interaction that could be achieved by minor monopole corrections in those multiplets that are experimentally not well determined in the benchmark nuclei used so far. Theoretical work in the framework of a general shell model study of the ^{78}Ni to ^{132}Sn model space is in progress [22].

This work is supported by the Spanish Ministerio de Educación y Ciencia under Contracts FPA2005-00696 and FPA2007-66069, the European Commission Contract 506065 (EURONS), the Swedish VR, EPSRC, and STFC (United Kingdom), the German BMBF, the Polish Ministry of Science and Higher Education (Grants 1-P03B-030-30 and 620/E-77/SPB/GSI/P-03/DWM105/2004-2007), and the Bulgarian Science Fund.

[1] J. Dobaczewski, I. Hamamoto, W. Nazarewicz, and J. A. Sheikh, Phys. Rev. Lett. **72**, 981 (1994).
[2] I. Dillmann *et al.*, Phys. Rev. Lett. **91**, 162503 (2003).
[3] J. Dobaczewski *et al.*, Phys. Rev. C **53**, 2809 (1996).
[4] J. M. Pearson *et al.*, Phys. Lett. **B387**, 455 (1996).
[5] T. Kautzsch *et al.*, Eur. Phys. J. A **9**, 201 (2000).
[6] A. Jungclaus *et al.*, Phys. Rev. Lett. **99**, 132501 (2007).
[7] M. Górska *et al.* (submitted for publication).
[8] T. Rodríguez, J. L. Egido, and A. Jungclaus, Phys. Lett. **B668**, 410 (2008).
[9] J. K. Hwang, A. V. Ramayya, and J. H. Hamilton, J. Phys. G **35**, 055102 (2008).
[10] A. Scherillo *et al.*, Phys. Rev. C **70**, 054318 (2004).
[11] N. Hoteling *et al.*, Phys. Rev. C **76**, 044324 (2007).
[12] H. Geissel *et al.*, Nucl. Instrum. Methods Phys. Res. B **70**, 286 (1992).
[13] J. Eberth *et al.*, Nucl. Instrum. Methods Phys. Res. A **369**, 135 (1996).
[14] J. Simpson, Z. Phys. A **358**, 139 (1997).
[15] S. Pietri *et al.*, Nucl. Instrum. Methods Phys. Res. B **261**, 1079 (2007).
[16] W. Andrejtscheff *et al.*, Nucl. Instrum. Methods **204**, 123 (1982).
[17] B. Fogelberg and P. Carlé, Nucl. Phys. **A323**, 205 (1979).
[18] B. Fogelberg, K. Heyde, and J. Sau, Nucl. Phys. **A352**, 157 (1981).
[19] R. Machleidt, Phys. Rev. C **63**, 024001 (2001).
[20] M. Hjorth-Jensen, T. T. S. Kuo, and E. Osnes, Phys. Rep. **261** (3&4), 125 (1995).
[21] ENSDF database (28/10/2008), http://www.nndc.bnl.gov/ensdf/.
[22] K. Sieja *et al.* (unpublished).
[23] E. Caurier, G. Martínez-Pinedo, F. Nowacki, A. Poves, and A. P. Zuker, Rev. Mod. Phys. **77**, 427 (2005).